The Mu2e experiment at Fermilab

C. Bloise, S. Bini, S. Ceravolo (Tech.), M. Cordelli (Ass. Senior),
E. Diociaiuti (AR), R. Gargiulo (Laur.), S. Giovannella,
D. Hampai, F. Happacher (Res.), M. Martini (Ass.),
S. Miscetti (Res.Naz.), D. Paesani (doct.), D. Pierluigi (Tech), B. Ponzio (Tech),
G. Pileggi (Tech), A. Russo (Tech), E. Sanzani (Laur.), I. Sarra .

1 Introduction

The most significant contribution of the LNF-INFN group for the Mu2e experiment is the design, prototyping, assembly and commissioning of the electromagnetic calorimeter, whose schematics and breakdown are shown in Fig. 1. The calorimeter is composed of two annular disks containing 674 pure CsI crystals each, with each crystal readout by 2 UV-extended Mu2e-SiPMs. A Mu2e SiPM is a custom-design array of six monolithic SiPMs cells of 6×6 mm^2 dimensions

At the moment of writing, the production phase of basic components (crystals and sensors) as well as the large mechanics parts is completed. The production of analog electronics is well underway while the digital electronics is starting. Due to pandemics, many operations were moved back to Italy and we delayed the assembly of components up to the summer of 2022. As a result, we have accumulated more than one year of delay in our scheduled target, that now foresees the calorimeter installed in the pit in 2024.

During 2022, Mu2e has achieved many important milestones but, due to the long delays introduced by COVID and by the construction of the magnetic system, it has been re-baselined, i.e. the US Department of Energy (DOE) has substantially refunded the experiment allowing O(10%) increase of the budget and a many years elongation of the schedule. The rest of the detector (Straw tube tracker and Cosmic Ray Veto system) are also suffering of delay but are in a good completion status.

2 Production status of the Calorimeter system

2.1 Read Out Units final characterization

Each calorimeter crystal is connected to an ensemble of Silicon photomultiplier and Front End Electronics (FEE) boards, named calorimeter Readout Unit or ROU. The exploded view of a ROU is shown in Fig. 2 and in more detail each unit is composed of:

- Two custom Mu2e SiPMs, each one made of the parallel of two series of 3 UV extended monolithic $6 \times 6\,\mathrm{mm}^2$ SiPMs.
- One copper holder on which the two Mu2e SiPMs are glued.
- Two custom FEE boards, one per Mu2e SiPM, connected via 4 pins directly to the SiPMs.
- One copper Faraday cage for shielding.
- One needle guide for the insertion of the optical fibers that will carry the light provided by the laser calibrating system.
- One reference guide and four screws to ensure the correct placement of the ROU on the support back plane in PEEK.

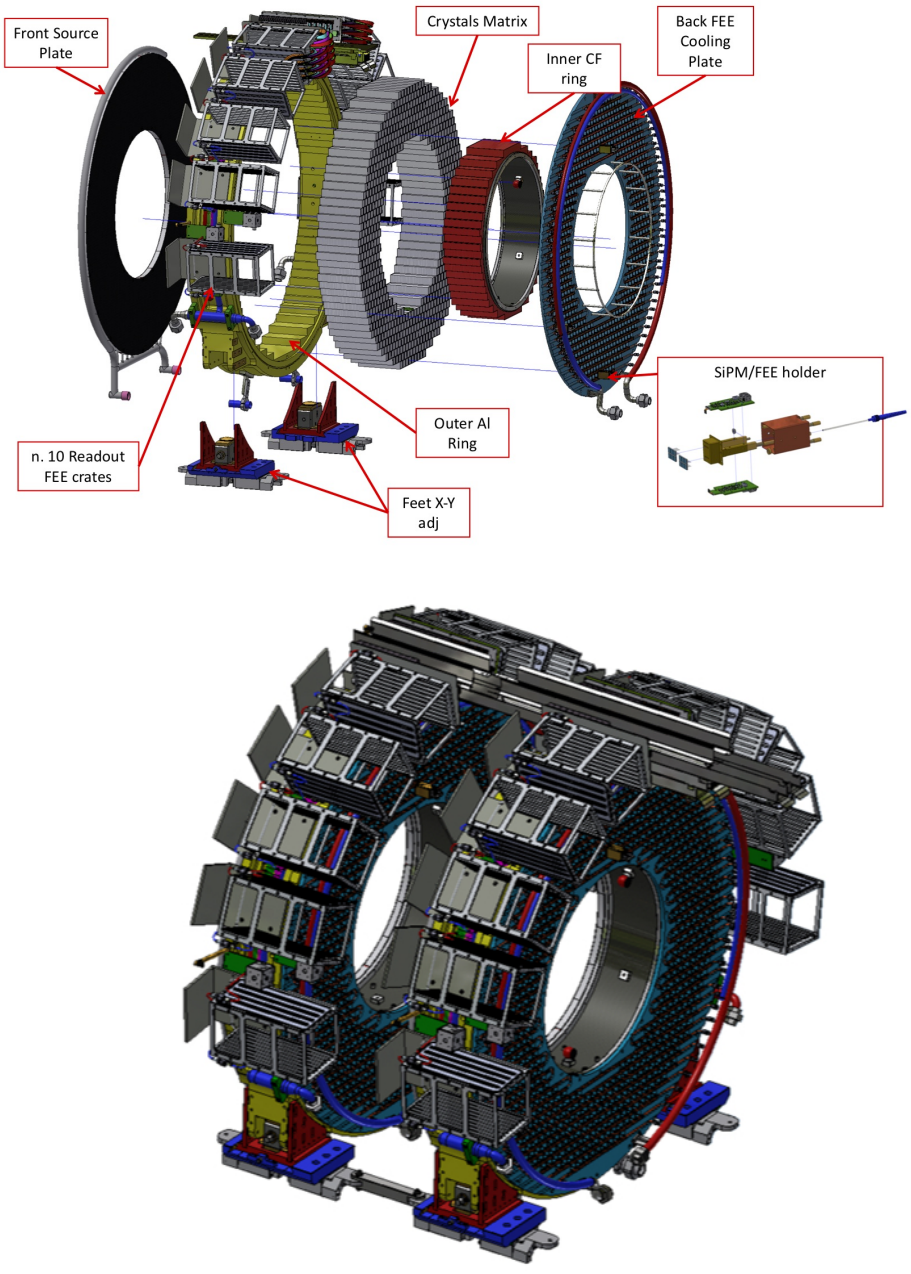

Figure 1: Exploded view of all the mechanical components and view of the two annuli on the detector train.

During 2022, $\sim$ 2500 calibrated FEEs have been assembled on the SiPMs' holder and underwent a final characterization test, to evaluate the gain of the complete read-out chain. At the moment of writing 840 ROUs have been shipped to Fermilab, out of which 674 have been already

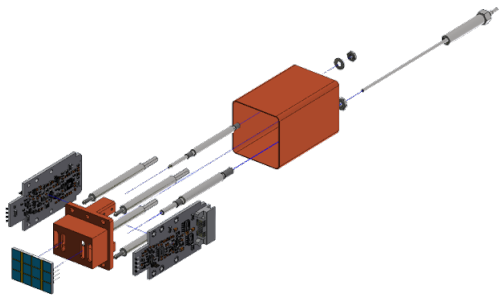

Figure 2: Exploded view of the components of a ROU.

installed on the first calorimeter disk assembled in SiDet. The remaining units are still under tests and are going to be shipped to Fermilab at the beginning of 2023.

2.1.1 FEE ADC and DAC calibration

The ROUs electronic slow control is realized by two specialized cards designed to operate in a master-slave configuration: the Mezzanine (MZB) and the Digitizer and Control (DIRAC) boards. The MZB provides the bias of the SiPMs and of the related slow control (voltage regulation, bias, etc.). A flash memory onboard the MZB stores calibration data in order to accurately set and monitor the SiPMs. To facilitate preliminary tests and calibration of the FEEs, an additional board has been designed to operate with a MZB and a DIRAC: the Active Load Board (ALB). The MZB can be connected to the ALB by means of a I2C serial communication bus. The ALB has three main functions:

- Read the high voltage (HV) applied to the FEE, as it appears at the SiPM pin connector.
- Set, change and read the source Load Current, i.e. the current sourced by the FEE HV bias regulator flowing through the SiPM pin connections.
- Evaluate the coefficients (offset and slope), in counts per physical unit or volts, of the ADC and DAC linear calibrations.

In this context, the most important calibration task is to determine the slope/offset coefficients of the ADC and DAC on-board of the single FEE. This can be done since the ALB can simulate any operative condition found when the FEEs will be populated with the SiPMs. These coefficients, which are slightly different for each FEE, can be stored in the MZB non-volatile flash-ROM, so that the MZB can precisely set the HV bias and translate the counts read from the ADC onboard of the FEEs into accurate estimates of the HV bias. A picture of the calibration setup is shown in Fig. 3, where also the detail of how the FEEs are connected to the ALB is presented.

2.1.2 The ROU Quality Control Station at LNF

In order to perform a quality control on the assembled ROUs, a Quality Control (QC) Station has been set up at LNF, as shown in Fig. 4. This setup work with two ROUs at the same time. A 420 nm blue LED at 10 kHz is used to illuminate the SiPMs. The light is attenuated through an automatic wheel with 9 positions, each one holding a neutral density filter with different attenuation value. The transmitted light is diffused uniformly on the SiPMs surface thanks to a box with sanded glass that also provides light tightness and allows to work in a controlled environment, thus

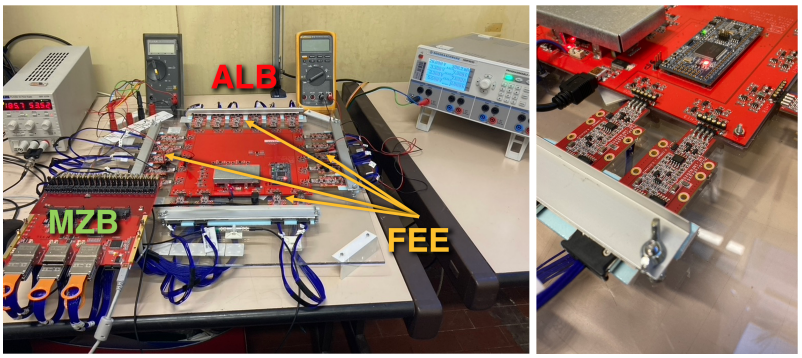

Figure 3: Left: Picture of the ALB setup. Right: Detail of the FEE connection to the ALB.

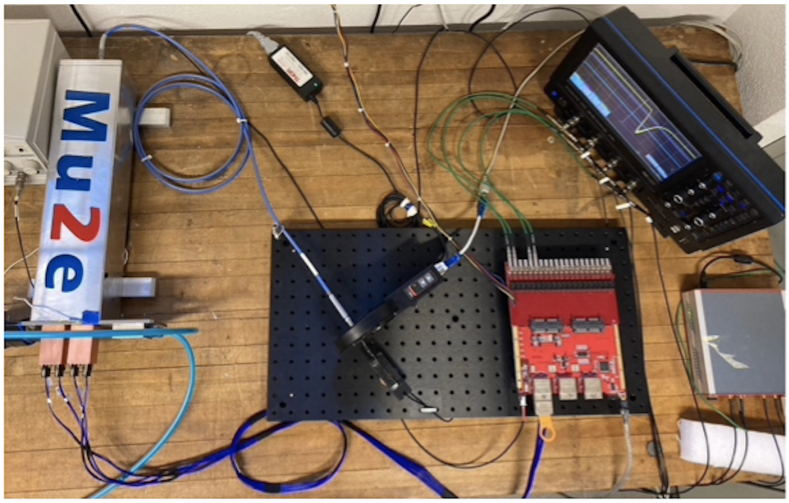

Figure 4: Picture of the QC Station.

ensuring good reproducibility of the measurements. The copper holders of the ROUs are screwed onto an aluminum plate that serves also as a conductive medium for temperature stabilization. A water chiller stabilizes the temperature around $\sim 25°C$, allowing to perform measurements in stable conditions and to have comparable results. Albeit this temperature stabilization, a residual variation of few degrees is still observed on the SiPMs, so we also record their temperature when making the test in order to perform a final offline gain correction as shown in Fig. 5 Left. The gain distribution at the end of the measurements is reported in Fig. 5 Right.

At the end of this calibration phase, we have observed a 1.5% reproducibility error, a channel by channel spread with an RMS lower than 5% and a temperature dependence of the gain of $O(3.5\%/°C)$.

2.2 Construction of the mechanical components and Dry run at LNF

The completion of the Construction Readiness Review in 2019 has sanctioned the maturity of the design and the technological choices, together with the executable drawings, of all the mechanical components of the Mu2e calorimeter. After the review we began the Procurement of all the main

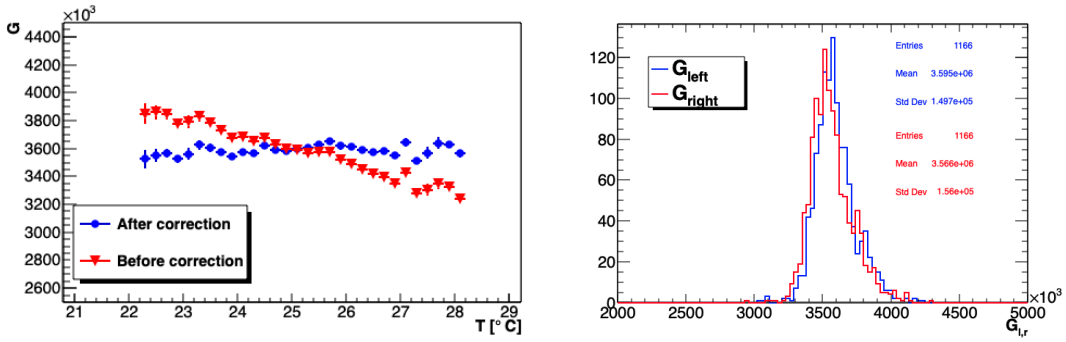

Figure 5: Left:Gain dependence on system temperature before(Red dots) and after (blue dots) the temperature correction. Right: ROU gains measured at V_{op}

mechanical parts that finished in 2022.

The detector is composed of two identical annuli with an Outer Radius of 1820 mm an Inner Radius of 336 mm and placed 700 mm apart along the Muon Beam line. As shown in Figure 1, each calorimeter annulus is composed of:

- an Outer monolithic stepped structural Al ring to house the parallelepiped crystals stack
- an inner Carbon Fiber and Al honeycomb mixture structural stepped ring;
- a pair of feet sitting on the detectors rail to allow also a X-Y adjustment;
- a Carbon Fiber and Al honeycomb front plate with an embedded pipes system for the flowing of a calibration radioactive fluorinert fluid;
- a PEEK back plate with apertures in correspondence of each crystal for the housing of the ROUs and with an embedded cooling circuit made of copper pipes;
- 10 digital electronic crates with a cooling serpentine connected to the main cooling pipes where digital electronics boards will be inserted (MZB + DIRAC).
- 674 CsI crystals wrapped with Tyvek and black tedlar;
- 674 ROUs;
- a secondary distribution system for the Laser calibration system.
- a lot of cables to connect ROUs to MZB, distributors for HV/LV cables and DAQ fibers.

During 2022 we kept interacting with the manufacturing companies, that had the individual tenders assigned, with all the quoted drawings to assess and agree on the best construction techniques. The manufactured components, before being shipped to Fermilab, were first assembled at LNF in a "mechanical dry run" to check the compliance to the design and ensure that the coupling of the separate parts was as planned. In this phase we could assemble the complete calorimeter structure and also define some details involving the routing of the FEE cabling and the needed supporting structure to hold the cables as well as the laser calibration fibers.

The last parts to be produced were the components made of composite material i.e. the inner stepped rings and the source plates. By the end of 2022 all the components of the first disk were shipped to FNAL, here we summarize the status of each component:

- concluded the production of the two outer cylinders made out of a monolithic Aluminum block to ensure maximum rigidity and resistance.
- concluded the construction of the FEE back plates. Also for these parts we have performed a Quality Assurance both checking the delicate geometry and leak and pressure testing the cooling circuit and the correct fitting of the SiPM holder in the plate apertures.
- finalized all the construction details of the Carbon Fiber parts. The construction of the stepped inner cylinders was successfully concluded. The stepped margin is a mixed sandwich of carbon fiber skins and Al honeycomb. After having lost a first shipment from USA, we have manufactured again at FNAL and shipped from there a new set of pipes of the two Source plates; the source system piping has been finally embedded in a Carbon fiber and Al honeycomb sandwich that corresponds to the calorimeter front plate.
- concluded the manufacturing of the two pairs of calorimeter disks feet components. These parts are still at LNF and need to be fully assembled before being shipped to FNAL.
- completed the construction of the crates that are housing MZB+Dirac electronic boards together with the purchase of 160 copper shield that will also dissipate power from the electronics.
- built all the components of the outgassing vessel and assembled it at FNAL. The setup was made fully functional so that we could perform the outgassing of all the components (crystals, ROUs, cables and boards) before assembling them on the disk.

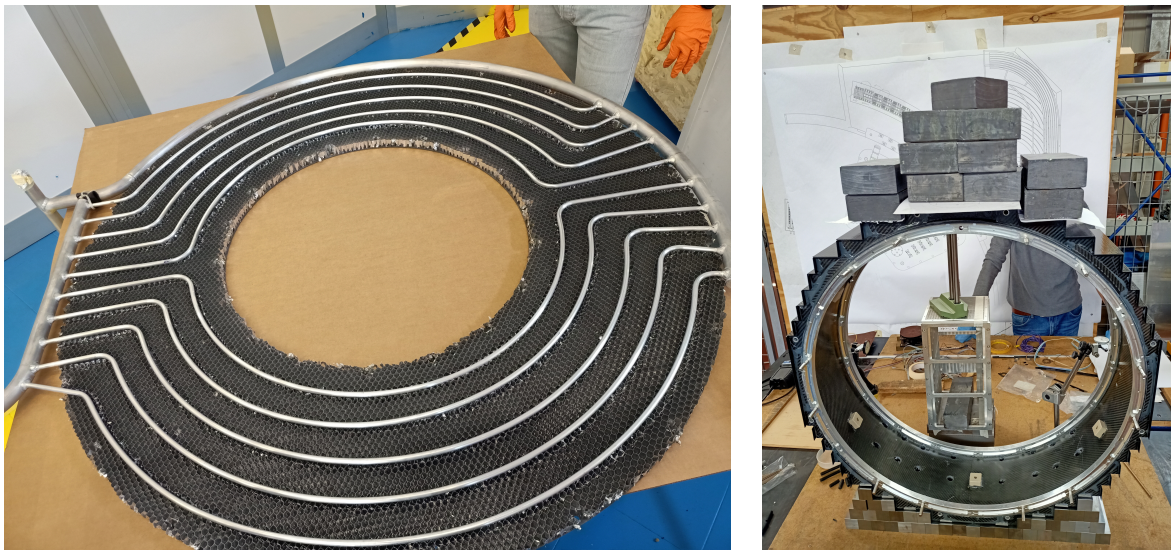

Figure 6: Source plate and pipe insertion; inner cylinder dead load test at LNF.

Figures 6 shows the front plate with the Al tubing for the source system inserted and the load test for the inner ring. The dry run test in the LNF Clean Room was performed to pre-assemble all the mechanics components before shipping them to Fermilab for final calorimeter assembly. We have assembled all the available mechanics component to check that the matching between parts is as designed. A lot of effort has been spent to perform the leak test of the cooling system: the main pipes running around the outer cylinder and connected through smaller pipes to the 10 Electronic crates installed on top of the Outer ring. Figure 7 shows two views of the assembled parts at LNF.

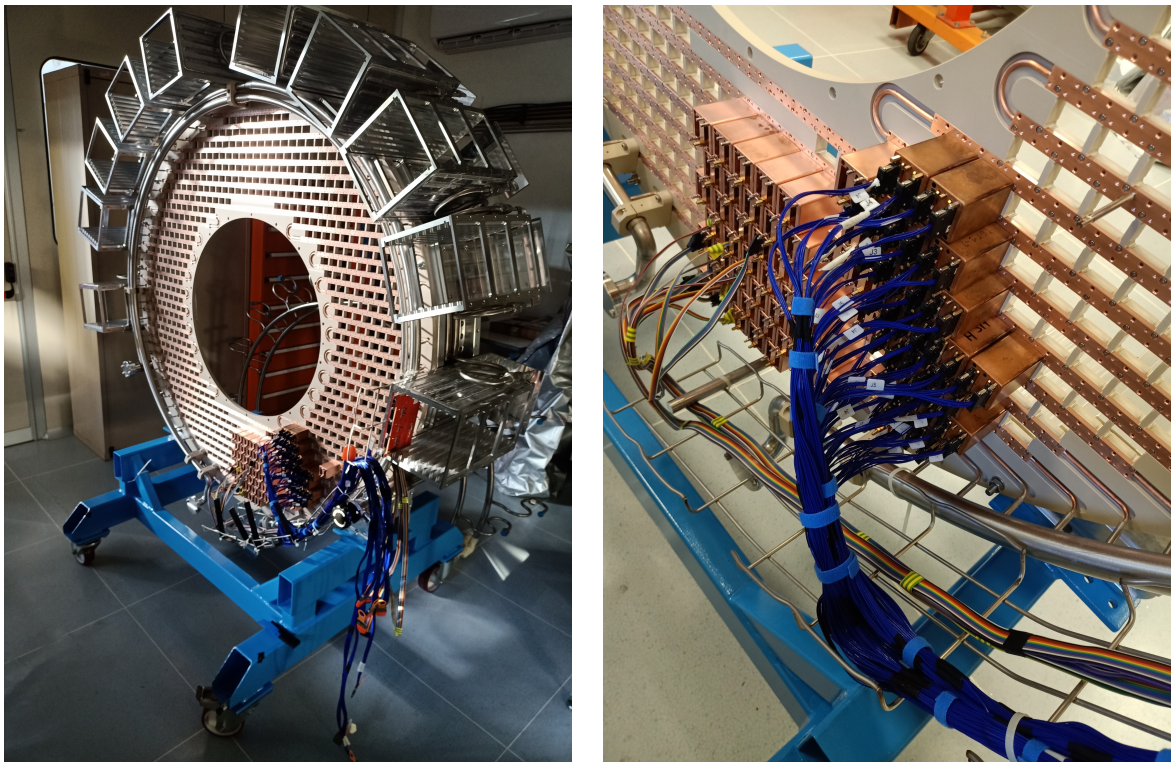

Figure 7: First Outer Cylinder installed on its assembly stand at LNF dry run (left) and cabling details (right).

2.3 First Calorimeter Disk Assembly

The first months of 2022 were dedicated to the completion of all the equipment necessary for the assembly of the first calorimeter disk and to the shipment of these parts from INFN to Fermilab. We shipped the FEE-cooling plates, the Carbon fiber (CF) source plates, the CF inner structural rings, all the Electronic crates and cooling pipes, all the Read Out Units, ROU's, completely assembled and tested with glued photosensors and read-out electronics on board. Once all the components arrived at Fermilab, we resumed traveling in crews to start the actual assembling of the first Calorimeter Disk. The assembly procedure consisted on:

- Placing the Outer Al ring on the stands and checking all the threads and geometry
- Installing the FEE plate onto the Outer ring
- Installing the Inner stepped CF inner ring
- Performing the first geometrical Survey of the Disk
- Stacking the crystals and perform a survey of their final position
- Closing the disk with the Source plate
- Installing cooling pipes and Electronic crates and pressure/leak test them
- Installing all the ROU

By December 20th the first calorimeter was fully instrumented and we could turn on the ROU and check the Cosmic ray output signals.

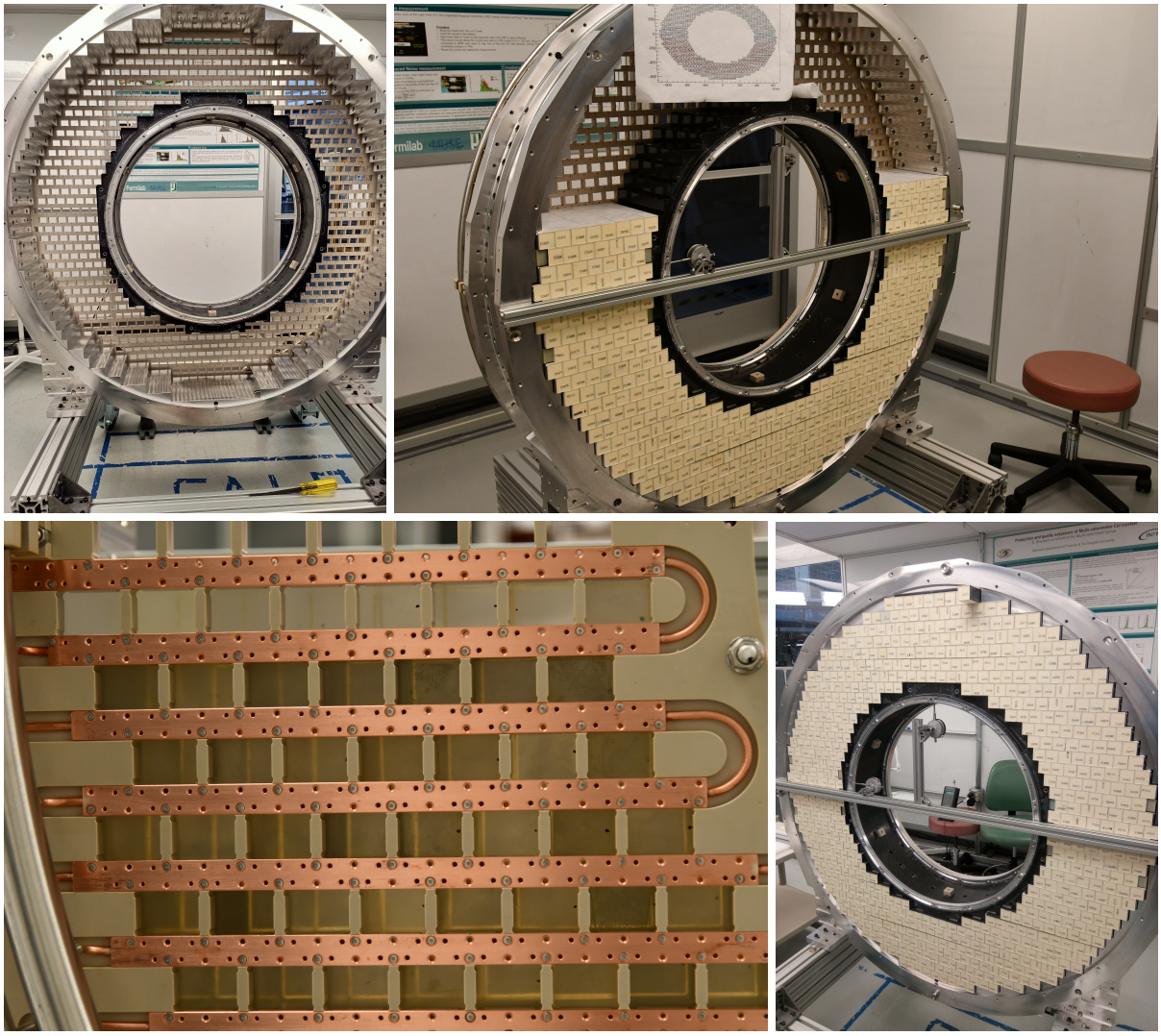

Figure 8: First Disk shell ready to be filled up with crystals and crystals stacking procedure details.

We have also Setup the Laser Calibration test stand and the secondary distribution system done with Optical fibers bundles and diffusive spheres. All tested channels were working fine. The tightness of the cooling lines have also been tested so that the next step will be to run the cooling system via a chiller that is being installed in the assembly room. The plan for the firs months of 2023 is the shipping from LNF of all the mechanical components and ROU's needed to assemble the second calorimeter disk, the outgassing of the crystals at Fermilab and the stacking of the crystals.

Figure 8 shows the first Calorimeter disk shell pre-assembled on the stand and ready to be filled with crystals. The growth of the crystal stack is also shown. Each layer of crystals has been surveyed and the planarity of each row accurately checked to match the crystal's face with the

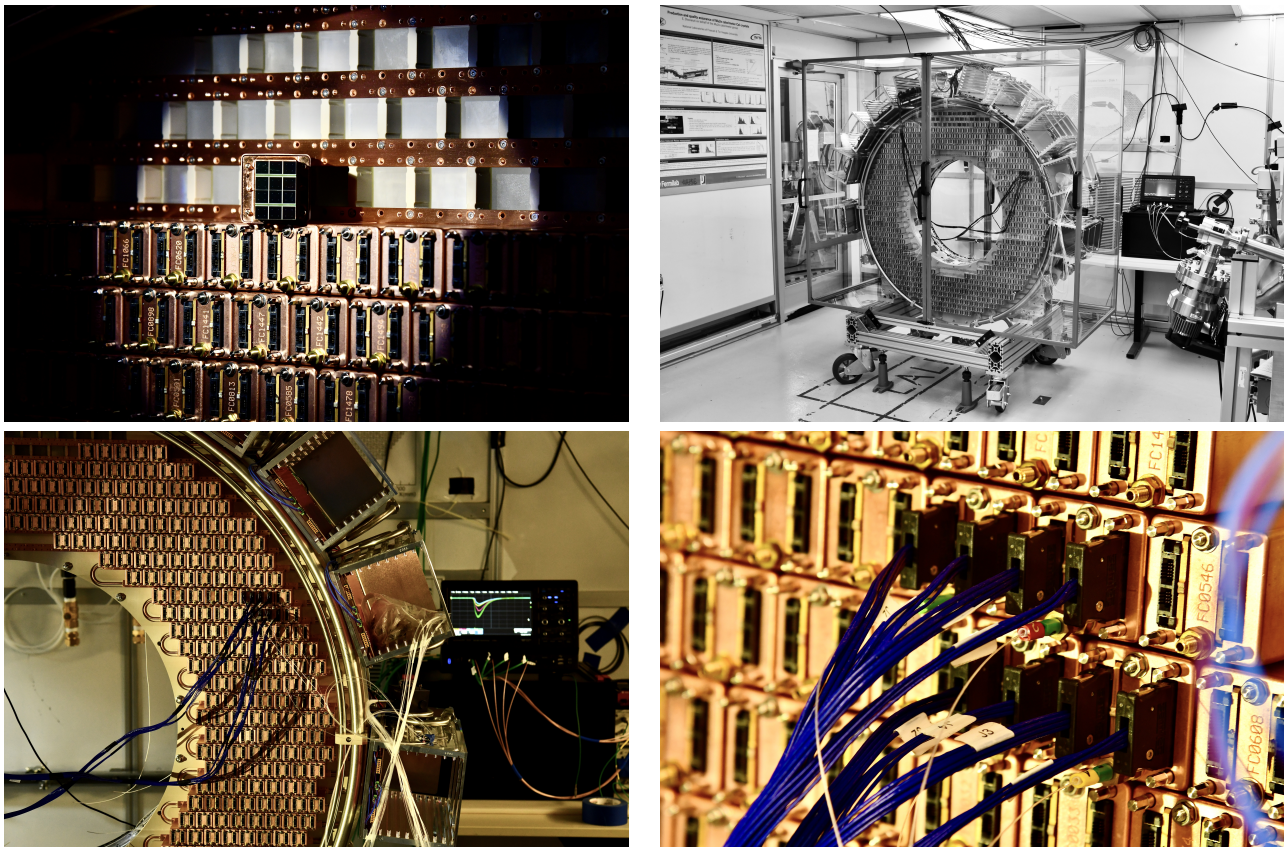

Figure 9: First Disk fully assembled of Crystals, enclosures, ROU's. First test of the channels using the laser calibration system.

FEE plate apertures.

3 Summary of Module-0 activities

A vertical slice test (VST) of the full calorimeter read out chain was performed with cosmic muons at LNF. For the VST, an electronics crate with a DIRAC and a MBZ board—and the respective cooling systems—were installed inside the Module-0 vacuum vessel to read out a total of 20 FEE channels. The 17 innermost crystals were instrumented with production ROUs, and a dual readout was used for the central and the central uppermost/lowermost crystals.

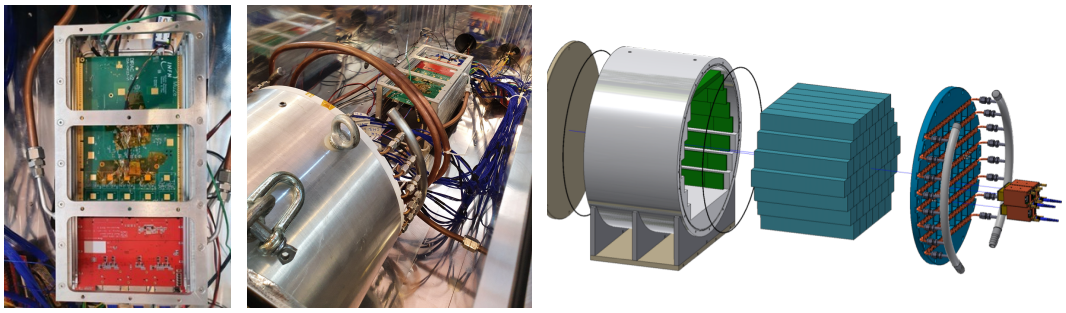

Figure 10: VST setup

Triggering was performed in various configurations, either via the coincidence of two scintillator plates placed above and below the Module-0, or via the DIRAC onboard autotrigger, for which a minimum hit number of three crystals was set. The energy response was equalised online acting on SiPM biases to a level ¡5 % and further offline equalisation was performed on the minimum ionizing particles (MIP) most probable 21 MeV deposit (Figure 11, left). The pedestals were characterised for all channels (Figure 12, right), yielding a ∼200 keV worst-case equivalent noise. The SiPM gain stability was checked against the MIP peak, and its fluctuations were compatible with the ±1 °C stability of the temperature regulation system (Figure 12, left).

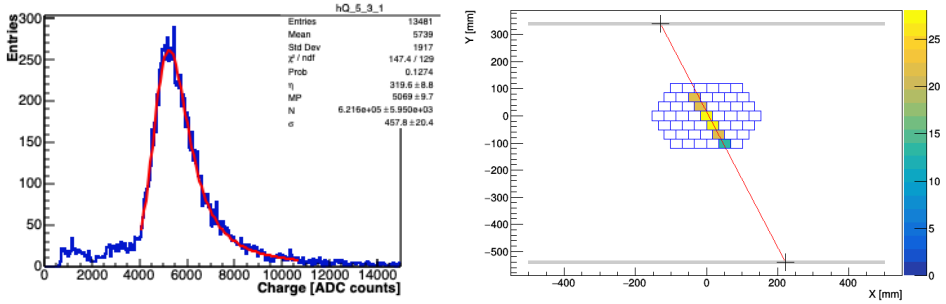

Figure 11: Example of MIP deposits in a crystal during VST with superimposed Landau–Gauss convolution fit (**left**). Example of MIP track reconstructed in the crystal matrix plane (**right**); colour scale represents energy deposit in MeV.

The MIP tracks inside the calorimeter were reconstructed with a 2D fit in the plane orthogonal to the crystal axes (Figure 11, right) and an iterative algorithm was used to calculate an energy-weighted time centroid for each event and adjust the relative timing offset between channels, accounting for the relative 2D time-of-flight (ToF) corrections, resulting in a relative alignment better than 5 ps RMS after five iterations (Figure 13, left). A mean time resolution of order 210 ps was evaluated with MIPs for individual crystals, from the time difference between the left and

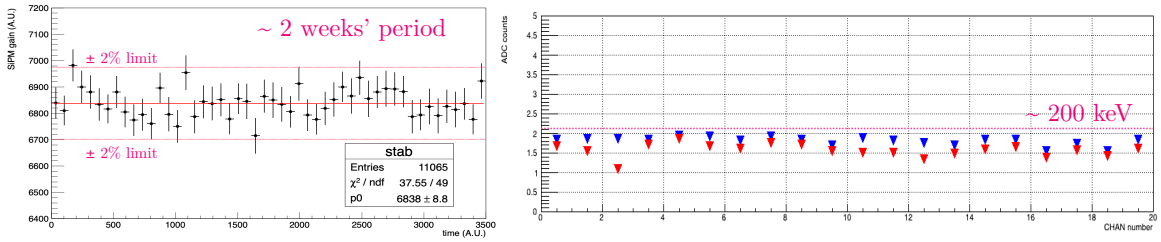

Figure 12: Relative SiPM gain stability over 2 weeks against MIP peak for the central channel (**left**). Charge pedestals expressed in ADC counts RMS for all Module-0 channels for two subsequent runs (blue and red colours).

right channels of the corresponding ROU, as shown for the central crystal in Figure 13, top-left.

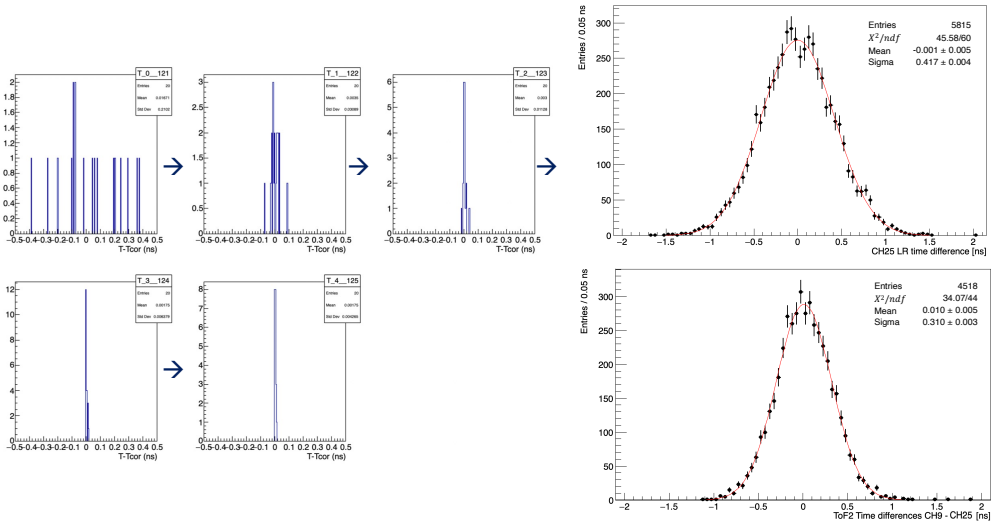

Figure 13: Overview of the timing alignment procedure (**left**): histogram of offset residuals after 5 iterations of the alignment algorithm. **Top-right**: example distribution of MIP timing differences between the left and right channels of the dual readout for the central crystal. **Bottom-right**: example of timing differences between two channels after 2D ToF correction and timing alignment

The timing difference distributions between channels, after ToF correction, were well centred around zero (Figure 13, bottom-left), and their sigma scales well within the quadrature sum of the individual timing resolution terms previously obtained, apart from a minor spread, associated to the ToF contribution due the unknown track slope along the calorimeter axis. An algorithm to reconstruct this slope from the optical transport timing differences on the crystal matrix is currently was developed for increased performance. The timing results were similar for the other instrumented channels. Finally, the mean timing resolution dependence on energy over the MIP energy range is shown in Figure 14 for the central channel.

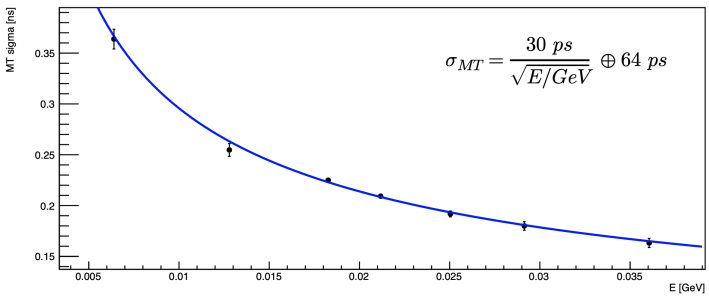

Figure 14: Central crystal mean time resolution for different energy slices (central channel).

4 Cosmic Ray Tagger for calorimeter pre-calibration

After completing their assembly at SiDet and prior to the installation in the detector solenoid, each calorimeter disk will be individually tested. Performance validation and reference calibration of the detector will be carried out using cosmic rays traced in 3D by means of a Cosmic Ray Tagger (CRT) system composed of two independent planar modules of scintillating counters. The two modules will be installed above and below the calorimeter disk under test and, in order to cover all disk volume, their axes will run orthogonally to the crystal ones.

Each module is composed of a single layer of 8 parallel EJ-200 scintillating bars, with a length of 1600 mm and a 15×25 mm^2 transversal cross-section. Each bar has a dual-side readout, and each side features a single Hamamatsu Mu2e SiPM connected to its own FEE board with a gain of 2. To enhance the modularity of the layout, each bar and its readout system were designed to be assembled as 16 individual units, as shown in figure 15. A total of 32 integrated optical couplers were manufactured in black acrylonitrile styrene acrylate (ASA), to allow a precise and robust alignment of the Mu2e SiPMs. The EJ-200 bars were wrapped with an internal 150 μm Tyvek layer, an external 500 μm Mylar foil and a final darkening tape layer. An external light-tight PVC box completes the assembly.

Figure 15: Pictures of one CRT module with the PVC light-tight box removed.

As a first characterisation, all measurements were carried out by selecting hits in the middle of the scintillator bars, so as to remove the effects of light attenuation and balance the dual-side readout response. Data taking was performed using an external trigger made of two 10 cm wide scintillators placed at the centre of one CRT module, orthogonally to the longitudinal direction of the bars. A Landau distribution is used to fit the charge spectrum, as shown in figure 16.

A template fit procedure was developed to reconstruct the timing of MIP signals and perform

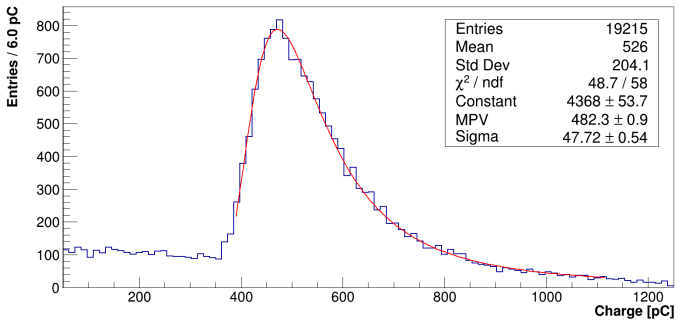

Figure 16: Charge distribution of one CRT channel (the other channels showing a very similar behaviour) fitted with a convolution of Landau and Gauss distributions.

the time-of-arrival hit position reconstruction along the bar axis. The time resolution dependence on the charge was then studied by dividing the timing data in charge slices, including both β and cosmic ray events collected at the centre of the bar under test. For each charge window, the time resolution was estimated with a Gaussian fit. The time resolution for a single photosensor $\sigma_t = \sigma_{\Delta t}/\sqrt{2}$ was fitted with a function including a constant term a, a stochastic term $b/\sqrt{Q}$ due to photostatistics and a c/Q term:

$$\sigma_t = a \oplus \frac{b}{\sqrt{Q}} \oplus \frac{c}{Q} \tag{1}$$

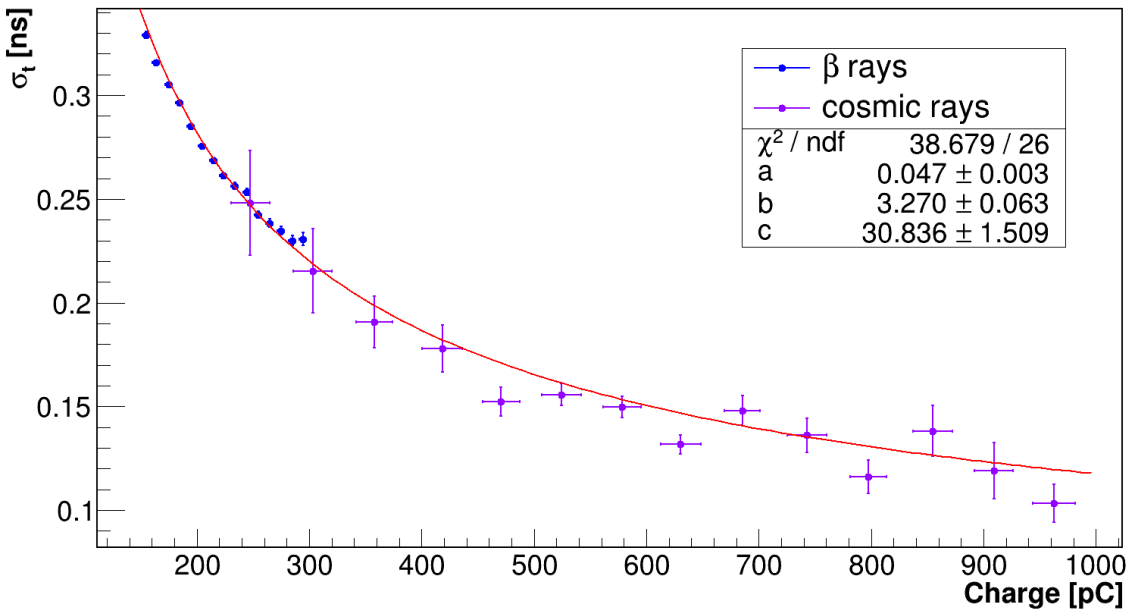

Figure 17: Fit of the time resolution with respect to the charge.

The constant term is around 47 ps, and the c/Q component is around 64 ps at MIP peak. A very good agreement is observed between the resolution determined with cosmic and β rays data.

The timing for each SiPM pulse is evaluated using the template fit procedure described in

the previous section. The hit position is then reconstructed from the difference between the light arrival time on the left and right SiPM: $T_L - T_R = \frac{2 \cdot z}{v_p} + \Delta T_{off}$ where v_p is the average light propagation speed inside the scintillating bars and ΔT_{off} is a residual time offset.

In order to estimate the dependence of the charge response with respect to the longitudinal position in the bars, the light attenuation in the scintillators was studied.

This behaviour is well modelled through the use of a bulk attenuation length (BAL), which corresponds to light propagating directly and depends only on material properties, and the technical attenuation length (TAL), which depends on the wrapping configuration of the scintillator. Therefore, the charge dependence along the bar is parametrised as follows:

$$Q(\Delta Z) = N \left(e^{-\frac{\Delta Z}{BAL}} + \frac{L_I}{L_D} e^{-\frac{\Delta Z}{TAL}} \right), \tag{2}$$

being ΔZ the distance of the hit position from the readout and $\frac{L_I}{L_D}$ the average ratio of indirect to direct light. For the EJ-200 scintillator, the BAL has a nominal value of 380 cm.

This analysis was performed with cosmic ray events collected using the two-modules setup, by fitting a Landau function to the core of the charge distribution and estimating the MPV for different slices of reconstructed position, as shown in figure 18.

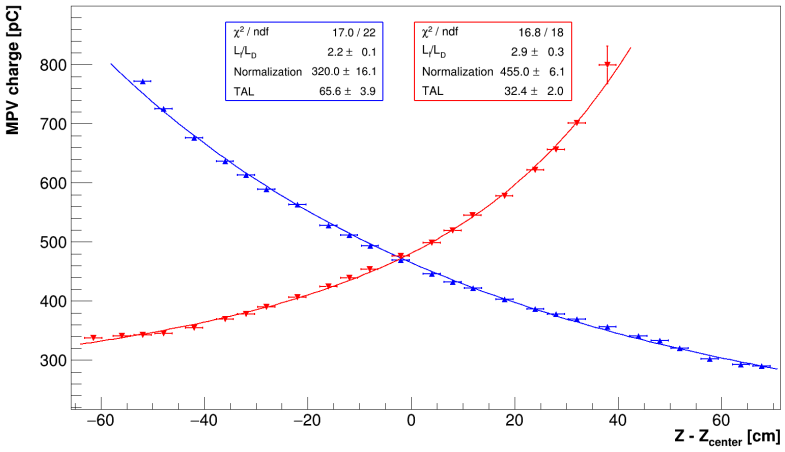

Figure 18: Light attenuation curve for cosmic ray events taken in auto-trigger. The curve is fitted with the function Q(Z) (see eq. 2). The results show an imbalance in the parameters values for the two sides, probably due to non-uniform wrapping or optical coupling.

A test with the complete setup was performed, by placing the two fully assembled and calibrated CRT modules one on top of the other, at a vertical distance ΔY of 10 cm . Only 4 bars per modules were tested, because of the limited number of digitiser channels available. In the final phase, before the installation of the calorimeter, two Mu2e DIRAC boards with a total of 40 readout channels will be employed to digitise all channels for the two CRT modules.

In this specific test, the trigger was based on the coincidence of pulses from one side of the top module and the opposite side of the bottom module, with a 130 pC (80 mV) charge threshold. In this configuration, the measurements are very clean because the environmental background is effectively removed, as shown in figure 19.

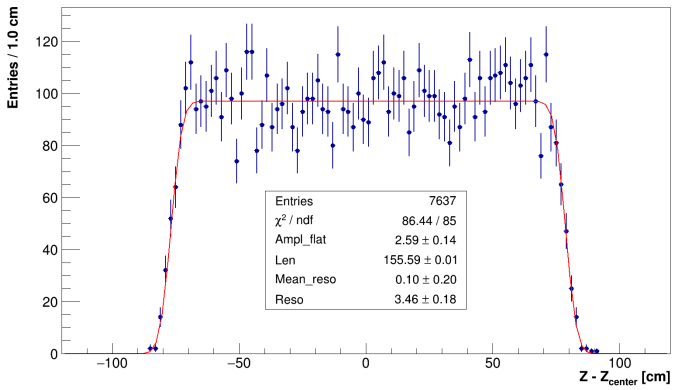

Figure 19: Distribution of $(Z - Z_{CENTER})$ with ΔY=10 cm.

4.1 Integration test with Module-0

A preliminary test of MIP tracking inside the Module-0 calorimeter prototype was performed. The two CRT modules were placed above and below the Module-0, with the scintillating bars orthogonal to the crystals, in order to track cosmic rays in both detectors (see figure 20).

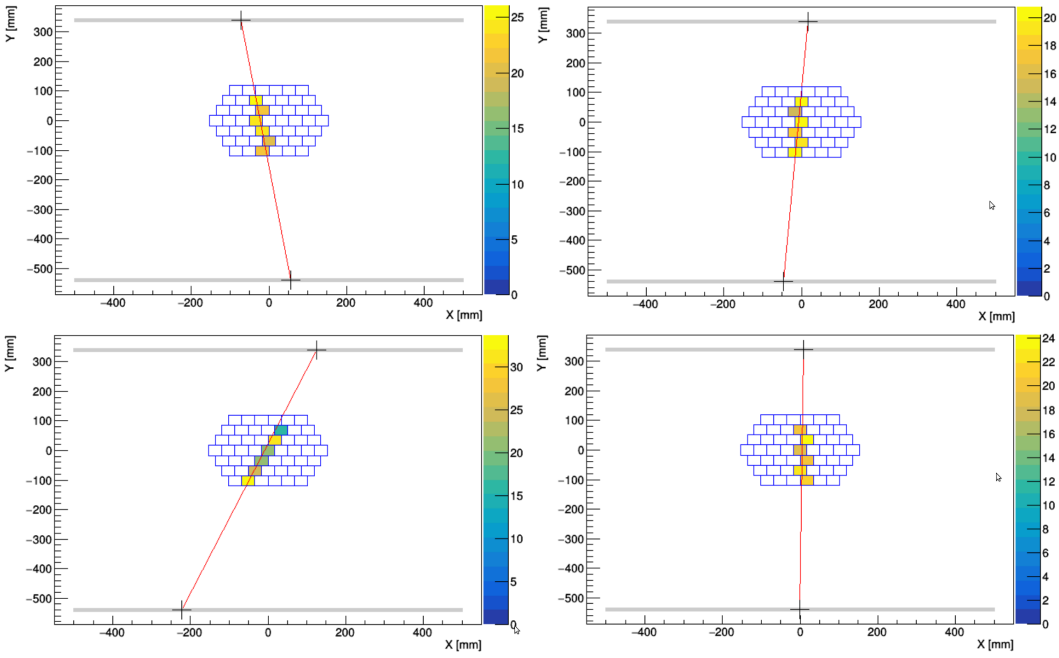

Figure 20: Examples of 4 cosmic ray tracks, traced in a vertical plane by both the CRT modules (in grey) and the Module-0 calorimeter prototype. The colour axis for the active crystals refers to the reconstructed deposited energy in MeV.

5 Detector Control System

Mu2e selected EPICS for the DCS Slow Control and monitoring software. EPICS is an open source framework originally developed at Argonne and Fermilab and now used in numerous experiments.

An Input Output Controller (IOC), running for each subsystem on a central DAQ server, will provide dedicated channels for all the monitored parameters. The IOC is a process that communicates with hardware and maintains Process Variables (PVs). A PV is a named piece of data associated with the detector electronics or hardware like temperature, voltage or current.A rack with 10 High Voltage and 10 Low Voltage Power Supplies (PS) is present at SiDet, Fermilab, in the mechanical assembly room. These PS will be the ones used to power each half of the calorimeter disks to carry out a cosmic ray data taking and fully survey the calorimeter and its electronics before moving it to the Mu2e Detector Hall.

An EPICS Input Output Controller (IOC) and Phoebus Graphic User Interface (GUI) have been developed in order to monitor the current and voltage of the PS. The number of PS under consideration can be increased simply changing one parameter, virtually making the produced GUI promptly ready for all the calorimeter power supplies. The GUI used at SiDet is shown in Figure 21.

Figure 21: Main GUI panel of the DCS for the PS at SiDet, in edit mode.

This preliminary test has proven that the DCS for the calorimeter power supplies is well underway. The next steps will consist on integrating this first version into the Mu2e DCS and Mu2e Web network for all calorimeter power supplies already installed in the Mu2e TDAQ room.

6 List of Conference talks and poster by LNF authors in Year 2022

1. F. Happacher, The Mu2e Experiment - Searching for Charged Lepton Flavor Violation, VCI 2022 - THE 16TH VIENNA CONFERENCE ON INSTRUMENTATION, Vienna (Austria)
2. F. Happacher, Mu2e Calorimeter Overview, Pisa Meeting on Advanced Detectors, La Biodola, Isola d'Elba (Italy)
3. E. Sanzani, An automatized QC station for the final calibration of the Mu2e Calorimeter SiPMs,Pisa Meeting on Advanced Detectors, La Biodola, Isola d'Elba (Italy)
4. R. Gargiulo, Design, assembly and operation of a scintillator based Cosmic Ray Tagger with SiPM readout Pisa Meeting on Advanced Detectors, La Biodola, Isola d'Elba (Italy)

5. S. Miscetti, Mu2e Calorimeter Overview, International Conference of Calorimetry in Particle Physics (CALOR 2022), University of Sussex (England)

6. D. Paesani, Mu2e crystal calorimeter front-end elecronics: design, characterization and radiation hardness, International Conference of Calorimetry in Particle Physics (CALOR 2022), University of Sussex (England)

7. D. Paesani,Design and construction status of the Mu2e crystal calorimeter, International Conference on High Energy Physics (ICHEP 2022), Bologna (Italy)

8. E. Sanzani, An automated QC station for the characterization of the Mu2e Calorimeter Readout Units, International Conference on High Energy Physics (ICHEP 2022), Bologna (Italy)

9. E. Diociaiuti, The Mu2e crystal and SiPM calorimeter, International Conference on Scintillating Materials & their Applications (Scint 2022), Santa Fe (USA)

10. S. Giovannella, Status of Mu2e/Comet experiments, Workshop on Flavour changing and conserving processes (FCCP-2022), Isola di Capri (Italy).

7 Publications

1. N. Atanov et al., "Development, construction and tests of the Mu2e electromagnetic calorimeter mechanical structures", Jinst, Volume 17, C01007 (2022).

2. N. Atanov et al., "Towards the construction of the Mu2e electromagnetic calorimeter at Fermilab", J. Phys.: Conf. Ser. 2374 012021 (2022).

3. K. Byrum et al,"Mu2e-II: Muon to electron conversion with PIP-II," [arXiv:2203.07569 [hep-ex]].

4. M. Aoki et al,"A New Charged Lepton Flavor Violation Program at Fermilab,"[arXiv:2203.08278 [hep-ex]].

5. N. Atanov et al., "The Mu2e Crystal Calorimeter: An Overview", Instruments, 6(4), 60 (2022).

6. N. Atanov et al., "Mu2e Crystal Calorimeter Readout Electronics: Design and Characterisation", Instruments, 6(4), 68 (2022).

7. F. Abdi et al.,"Mu2e Run I Sensitivity Projections for the Neutrinoless $\mu^- \to e^-$ Conversion Search in Aluminum," [arXiv:2210.11380 [hep-ex]].

8. N. Atanov et al., "Development and construction status of the Mu2e electromagnetic calorimeter mechanical structures," JINST **17** (2022) no.10, C10021

9. C. Bloise et al., "An automated QC station for the characterization of the Mu2e Calorimeter Readout Units," PoS **ICHEP2022**, 336

10. C. Bloise et al.,"Design and construction status of the Mu2e crystal calorimeter," PoS **ICHEP2022**, 314

8 Theses

1. Ruben Gargiulo, "Design, Calibatrion strategies and commissioning of the Mu2e Calorimeter", thesis in Laurea Magistrale at "La Sapienza University", Rome, 30/09/2022.

2. Elisa Sanzani," Quality Controls for the Mu2e calorimeter and R&D studies for the Muon Capture Rate determination", thesis in Laurea Magistrale at "Bologna University", Bologna, 28/10/2022.